Phase Diagram And Adsorption-Desorption Kinetics Of CO On $Ru(0001)$: Present Limitations Of A First Principles Approach

J.-S. McEwen*
Department of Physics and Atmospheric Science, Dalhousie University, Halifax, Nova Scotia, Canada, B3H 3J5

A. Eichler
Institut für Materialphysik and Centre for Computational Materials Science, Universität Wien, Sensengasse 8/12 A-1090 Wien, Austria

(Dated: February 2, 2008)

A lattice gas model is used to study the equilibrium properties and desorption kinetics of CO on Ru(0001). With interactions obtained from density functional theory (DFT) the phase diagram and temperature programmed desorption (TPD) spectra are calculated up to a coverage of 1/3 ML using top sites only. For coverages beyond 1/3 ML hollow sites are included. Good agreement is obtained between experiment and theory for coverages below 1/3 ML using top sites only. When including hollow sites, DFT calculations fail in predicting the correct binding energy differences between top and hollow sites giving disagreement with TPD, low energy electron diffraction (LEED) and heat of adsorption experiments.

PACS numbers: 02.70.Wz, 05.50.+q, 31.15.Ew, 68.35.Md, 68.43.Bc

I. INTRODUCTION

Adsorbate systems with commensurate structures can be described successfully with a lattice gas model with one or more adsorption sites. The energetics are contained in a few parameters such as binding energies, vibrational frequencies and lateral interactions. In a "complete" theory these parameters would be obtained from first principles quantum mechanical calculations, for instance based on density functional theory. This has been demonstrated successfully for oxygen on Ru(0001) for both equilibrium and desorption kinetics [1, 2]. An attempt to repeat such an approach for CO/Pt(111) has been shown to fail [3], most importantly due to the fact that DFT does not produce the right energetic order of the binding sites for many transition and noble metal substrates [4, 5, 6]. Nevertheless a satisfactory explanation of all available equilibrium and kinetic data could be achieved by treating a minimal set of the lattice gas parameters as phenomenological fitting parameters [3]. In this paper we will show that for CO/Ru(0001) DFT yields parameters that give a good account for data below 1/3 ML provided only top sites are included, but fails when bridge and hollow sites come into play.

Let us begin with a quick survey of the experimental data needed to model this system appropriately; details and actual data will be given later. At low coverage ($\theta \leq 1/3$ ML) and temperature (T < 150 K) CO binds to on-top adsorption sites only resulting in a $(\sqrt{3} \times \sqrt{3})R30°$ ordered structure at 1/3 ML [7, 8, 9, 10]. As the coverage is increased beyond 1/3 ML three fold hollow sites become occupied forming a $(2\sqrt{3} \times 2\sqrt{3})R30°$ structure at 1/2 ML, with equal population of top, hcp and fcc sites, for which two different geometries have been proposed [11, 12]. For coverages beyond 1/2 ML, a p(7×7) structure at 0.55 ML with top and bridge sites [11] and a $(2\sqrt{3} \times 2\sqrt{3})R30°$ structure at 7/12 ML [11, 12] have been suggested. Finally, a $(5\sqrt{3} \times 5\sqrt{3})R30°$ saturation structure at 49/75 ML was observed using He scattering experiments [13]. A summary phase diagram was given by Pfnür *et al.* [12]. Equilibrium isobars and the isosteric heat of adsorption [14] have been measured, too, as well as the temperature programmed desorption spectra [14, 15]. The sticking coefficient was measured directly with molecular beam scattering as a function of temperature, coverage and kinetic energy of the incident beam [15] and by coverage vs. exposure curves [16]. Measurements have also been done for the CO stretch frequency using infrared reflection-adsorption spectroscopy (IRAS) [10, 17, 18]. The other frequency modes of the on top species have been determined using helium scattering experiments [13] and IRAS measurements [19].

In the next section we briefly introduce the lattice gas model, the DFT setup as well as the methods used to calculate the equilibrium and kinetic data. In section 3 we consider the modeling of CO/Ru(0001) with top sites only up to 1/3 ML and in section 4 we show and discuss the modeling of this system with top and hollow binding sites up to 1/2 ML. The paper ends with a discussion to what extent present DFT methods can be used to model CO/Ru(0001).

*Electronic address: mcewenj@fizz.phys.dal.ca

II. THEORETICAL METHODS

A. Lattice gas formalism

To set up a lattice gas model for CO/Ru(0001) we require a Hamiltonian, which we write down for top sites only as:

$$H = -(V_0 + k_B T \ln(q_3 q_{\rm int})) \sum_i t_i + \frac{1}{2}\sum_n^3 \sum_i \sum_{a_n} V_n t_i t_{i+a_n} + \frac{1}{3}\sum_i \sum_{a,b} V_{\rm trio} t_i t_{i+a} t_{i+b} \quad (1)$$

with obvious generalizations to a multi-site system [1, 3]. Here the sum on i exhausts all lattice cells; $i + a_n$, $i + a$ and $i + b$ label neighboring cells and we have introduced occupation numbers $t_i = 0$ or 1 depending on whether a site in cell i is empty or occupied. V_0 represents the depth of the adsorption potential well with reference to the gas phase molecule. Moreover, V_1, V_2 and V_3 denote first, second and third nearest neighbor interactions respectively. $V_{\rm trio}$ includes V_{lt}, V_{bt}, V_{tt} which denote linear, bent and triangular trio interactions involving first and sometimes second nearest neighbor interactions [1, 3]. Furthermore, $q_3 = q_{\rm z} q_{\rm xy}$ is the vibrational partition function of the adsorbed molecule for its center of mass vibrations with respect to the surface with $q_{\rm z}$ being the component perpendicular to it. Likewise, $q_{\rm xy}$ is the partition function for the motion parallel to the surface. We have also allowed for the fact that the internal partition for rotations and vibrations of an adsorbed molecule is changed from its free gas phase value, $Z_{\rm int}$ to $q_{\rm int}$, if some of the internal degrees of freedom are frozen out or frustrated [20].

We determined the temperature-coverage phase diagram by calculating the corresponding $(\sqrt{3}\times\sqrt{3})R30^\circ$ order parameter [21]. Second order phase transitions were defined at a given temperature by the inflection point of the order parameter [22, 23] as a function of the chemical potential. First order phase transitions were marked when it was discontinuous [23, 24]. To calculate the resulting TPD spectra we used the theoretical framework described in [20]. The desorption rate depending essentially on the sticking coefficient $S(\theta, T)$ and the chemical potential of the adsorbate $\mu(\theta, T)$ (which includes its binding energy and the frequencies of the CO molecule in the gas phase and on the surface).

B. Monte Carlo Methods

The TPD, isobars and the phase diagram were calculated with Monte Carlo methods. Simulations were performed in both the grand canonical and canonical ensembles (chemical potential and coverage specified, respectively) using the Metropolis algorithm (with spin flip and infinite Kawasaki dynamics) [25]. Equilibration times of the order 2^{14} up to 2^{18} Monte Carlo sweeps were allowed for each coverage or chemical potential point. When dealing with top sites only, we initialized the system in a $(\sqrt{3}\times\sqrt{3})R30^\circ$ structure for the first temperature-coverage, temperature-chemical potential point, respectively. For coverages beyond 1/3 ML, we occasionally initialized the system with a p(2×2) structure (with equal populations of top and hcp sites at 1/2 ML) or with a clean substrate. Thereafter, to fasten equilibration, initialization of the system occurred with the final configuration of the previously calculated point. When calculating the phase diagram, we performed averages over a maximum of five independent samples. For the canonical ensemble, the particle insertion method of Widom [26] was used in order to calculate the chemical potential with Monte Carlo methods; a method which was developed to be applicable especially for the interaction parameters derived from DFT calculations. To allow adsorption on hollow and top sites we used three interpenetrating 42×42 or 60×60 lattices, with periodic boundary conditions. This lattice size was chosen to allow commensurate low-coverage ordered structures with periods of 3 and 6.

C. Density Functional Theory setup

We have calculated all necessary interaction parameters with the Vienna ab initio simulation package VASP [27, 28, 29], a plane-wave DFT program, which is based on the projector augmented wave method [30]. A cutoff energy for the expansion of the plane waves of 400 eV was found to be sufficient for an accurate description. For exchange and correlation the generalized gradient approximation (GGA) according to Perdew et al. [31] was applied. The surface was modeled in $p(2\times2)$ and $p(3\times3)$ cells at the theoretical lattice constant of a=2.725 Å and c/a=1.579, with slabs consisting out of 6 layers, of which the uppermost two layers were structurally optimized where mentioned in the text. The Brillouin zone was sampled by a grid of $(3\times2\times1)$ k-points.

The adsorption energy for an isolated CO molecule $(-V_0)$ is defined as the adsorption energy for 1/9 ML coverage $(E_a^{\theta=1/9})$ derived from the total energies of the adsorbate/substrate system $(E_{total}^{CO/Ru})$, the bare surface (E_{total}^{Ru}) and the free CO molecule (E_{total}^{CO}):

$$-V_0 = E_a^{\theta=1/9} = E_{total}^{CO/Ru} - E_{total}^{Ru} - E_{total}^{CO} \quad (2)$$

The interaction parameters where determined by calculating the energy of the system for ten configurations at various coverages between 1/9 and 1 ML [1]. The energy of the system at a coverage of 1 ML was calculated twice: once with the (3×3) unit cell and again with a (2×2) unit cell. Consequently, all our interaction sets had more ordered structures than lattice gas Hamiltonian parameters so that we have fitted, using a least squares procedure, for the resulting interactions. Maximum

deviations from the calculated energies of the ordered structures with respect to what was obtained from the interaction parameters, were never greater than 5 meV.

III. MODELING WITH ON-TOP SITES AT LOW COVERAGE

CO/Ru(0001) has already been modeled successfully in the past using a lattice gas model with top sites only. The interaction and binding energy parameters were obtained phenomenologically by matching the phase diagram [32], the TPD spectra and the isosteric heat of adsorption [33].

In this work, three strategies were used to obtain these energies:

- In the first (*method A*) the top two layers of the bare substrate were completely relaxed and then kept fixed at these positions for the description of CO adsorption. The geometry of the adsorbed CO molecule was optimized only for the 1/9 ML configuration. For higher coverages, the same CO bond length and adsorption height was used.

- In *method B* the position of the CO molecules as well as the first two layers of the substrate were allowed to relax for all of the ordered structures.

- For comparison, we have also looked at the resulting interaction parameters when fixing laterally the CO molecules for the structure at 2/9 ML (which is the only configuration for which lateral forces on the CO molecule are symmetrically allowed) with all the other ordered structures fully relaxed (the CO molecules and the first two layers of the substrate). This third approach (*method C*) was used for O/Ru(0001) [1].

In Table 1, we show the resulting energies using all of the above three methods together with the standard deviation σ describing the average deviation between the calculated energies and the parametrization. We used the minimum number of parameters so as to have an acceptable value of σ. These interaction sets show that the second neighbor interaction between top sites, V_2, is repulsive for the relaxed calculations. This is clearly at odds with the experimental phase diagram which implies a coexistence between the $(\sqrt{3}\times\sqrt{3})R30^\circ$ structure and a lattice gas, and requires V_2 attractive. In addition, the calculated TPD spectra using transfer matrix techniques with method B and C give low initial-coverage spectra peak positions that do not correspond to experiment and are much too broad. On a more positive note, the first neighbor interaction between ontop sites for method B (cf. Table I) is closer to what was obtained by previous phenomenological models of this system using only one binding site [33].

Interestingly, for method C V_2 becomes negative (-6 meV) if the same set of parameters (V_1, V_2, V_{lt}, V_{tt}) is used as for method A. However, in this case the standard deviation increases significantly to 19 meV.

Because of this obvious discrepancy for the relaxed calculations, we restrict the further analysis, to the results obtained within method A. The reason for this behavior can be found probably in local relaxations for specific configurations used for the determination of the parameters, which are not representative for the interaction of CO on Ru(0001) in general. For the unrelaxed setup in method A, the CO molecule and the surface is treated completely identically in all configurations, entirely in the spirit of the lattice gas like interaction. For the relaxed setups, however, the number of input configurations would probably have to be increased such that relaxation effects, which are only characteristic of one specific arrangements of molecules, but not of the interaction between molecules itself, are averaged out.

The resulting phase diagram and TPD spectra with the parameters of method A are given in Fig.1 and show reasonable agreement with experiment provided we lower the binding energy of a single CO molecule by -174 meV (our unadjusted binding energy places the model curves 55 K too high). The experimental sticking coefficient was used [16]. Even with this adjustment there is still some disagreement for the spectra with an initial coverage of 1/3 ML. One way to correct for this would be to allow for hollow sites in our model for which there would be a small but finite number around these temperatures and coverages.

The phase diagram calculation does not depend on the binding energy of the top sites. It is dominated by two phases, the $(\sqrt{3}\times\sqrt{3})R30^\circ$ structure, which saturates at 1/3 ML and a non-ordered lattice gas (l.g.) phase. To access the high temperature part of the phase diagram experimentally would require pressures up to 10^{-4} mbar, which is not accessible with LEED [8]. It has in fact been predicted that T_c must be at least 550 K at 1/3 ML. This is in agreement with our calculations, which predict an order disorder temperature of 1000 K at 1/3 ML under the restriction of on top adsorption only. We remark that this value will be considerably lowered if there is a spillover into other types of binding sites for coverages beyond 1/3 ML, resulting in a continuous reduction in temperature (and chemical potential) of the hight of the order phase boundary around 1/3 ML. Moreover, the value of V_2 can be directly read from the experimental phase diagram [32] with the value of the tricritical point given by $\approx 1.06V_2$. Experimentally, the tricritical point is around 150 K [12] for which there is some evidence from slow diffusion of the CO molecules [8]. This could be the source of the small discrepancy between our calculations and experiment for the first order transition points.

From these comparisons with experiment we can conclude that DFT does reasonably well in at low coverage ($\theta < 1/3$ ML) and since even in this coverage regime hollow sites come into play at high temperatures

TABLE I: Interactions energies (eV) derived within the DFT framework with three different strategies (A,B,C, cf. text) for the CO/Ru(0001) system for top sites together with the corresponding standard deviation (σ). E_{top} denotes the binding energy of the top site, the definition of the interaction parameters is given in the text.

Method	E_{top}	V_1	V_2	V_3	V_{lt}	V_{bt}	V_{tt}	σ (meV)
A	-1.796	0.230	-0.010	-	-	0.010	-0.048	3
B	-1.948	0.137	0.002	0.022	0.104	0.066	-0.231	2
C	-1.948	0.263	0.002	0.022	-0.021	0.004	-0.042	2

(T > 150 K) it does even better at low temperature. Similarly, the adsorption isobars at 1.3×10^{-4} mbar and 1.3×10^{-6} mbar are limited to 1/3 ML for T > 400 K.

Moreover, one may question the relevance of incorporating trio interactions for coverages below 1/3 ML. Indeed, with such a large nearest neighbor interaction these trios will practically never occur below 1/3 ML, even at desorption temperature and despite the attractive triangular trio interaction. However, fitting the calculated energies with V_1 and V_2 alone using method A results in $V_1 = 0.216$ eV and $V_2 = -0.060$ eV with $\sigma = 4$ meV. This would give a phase diagram similar to that given in Fig. 1 but with a tricritical point that one can estimate [32] to be 75 K instead of $\sim$ 120 K as shown in Fig. 1. For coverages beyond 1/3 ML, it is quite plausible that trio interactions become important. Indeed, this would help to explain the asymmetry in the experimental phase diagram. However, as been noted before, the asymmetry of the phase diagram can be explained either with a spillover into other binding sites [22] or with trio interactions [2], but it is quite possible that there is a combination of both. Since from the experimental data we know that a spillover must occur for coverages beyond 1/3 ML one cannot argue from symmetry arguments alone that one must have trio interactions. This makes it necessary to analyze the experimental data for coverages beyond 1/3 ML to consider the relevance of trio interactions for this system. With all of these facts in mind, we now proceed to model the adsorption behavior at higher coverages.

IV. MODELING WITH ON-TOP, HCP AND FCC SITES

The interaction energies between sites of the same type for fcc and hcp sites were calculated with the same procedure as for the top sites. For the same reason as for the low coverage regime, we present here the results of method A only. In addition, we show in Table II the adsorption energies per CO molecule for all investigated structures. These results are in line with previous DFT calculations that predict that the top sites are the most favorable binding site at low coverage [34, 35]. We note that the energy for the (1×1)-CO structure using a (2×2)

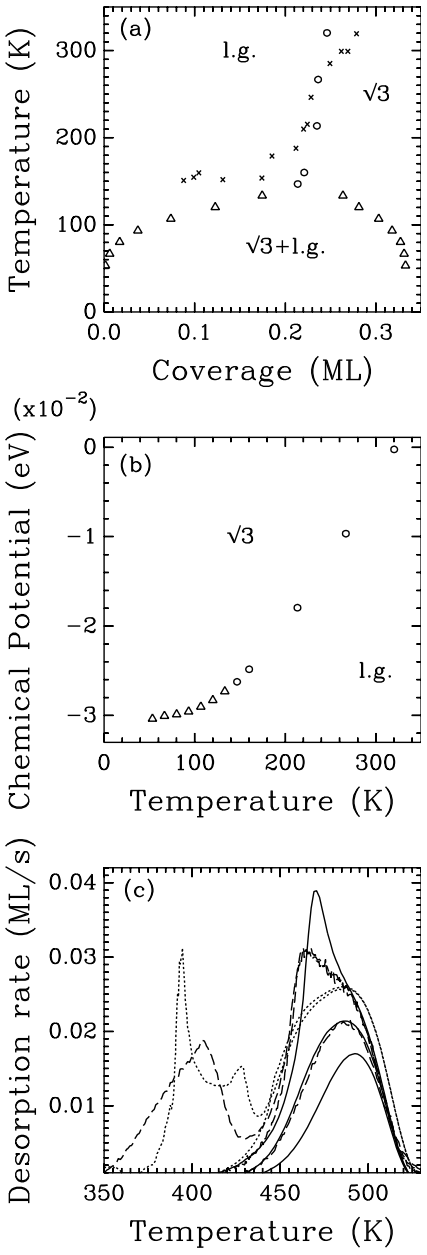

FIG. 1: (a) Phase Diagram up to 1/3 ML in the temperature-coverage plane using the lattice gas model with top sites only on a 60×60 lattice (interactions from method A, cf. Table 1). The crosses are the experimental points [12], the circles indicate second order phase transitions, the triangles first order transitions between lattice gas (l.g.) and $(\sqrt{3}\times\sqrt{3})R30^\circ$ ($\sqrt{3}$) phases. (b) The corresponding phase diagram in the chemical potential-temperature plane. (c) The predicted temperature programmed desorption spectra using the experimental sticking coefficient [16] and a heating rate of 5 K/s at initial coverages of 0.33, 0.25 and 0.15 ML with the top site only model (solid), the experimental spectra at 0.50, 0.33 and 0.22 ML (dashed) [15] and the spectra with the top and hollow site model at 0.50 and 0.33 ML (dotted). The theoretical curves have had their binding energy adjusted by -174 meV in order to aid the comparison with experiment.

TABLE II: Calculated adsorption energies (eV) for CO/Ru(0001) per CO molecule with method A (cf. text).

site	$E_a^{\theta=1/9}$	$E_a^{\theta=2/9}$	$E_a^{\theta=1/4}$	$E_a^{\theta=1/3}$	$E_a^{\theta=1/2}$	$E_a^{\theta=2/3}$	$E_a^{\theta=3/4}$	$E_{a,(2\times2)}^{\theta=1}$	$E_{a,(3\times3)}^{\theta=1}$
top	-1.796	-1.686	-1.793	-1.827	-1.572	-1.452	-1.371	-1.172	-1.176
hcp	-1.750	-1.635	-1.774	-1.755	-1.509	-1.389	-1.281	-1.118	-1.127
fcc	-1.672	-1.557	-1.660	-1.676	-1.426	-1.323	-1.231	-1.097	-1.104

and a (3×3) unit cell differ by 7 meV for fcc sites and 9 meV for hcp sites. When determining the corresponding interactions, we needed to include linear trios as well as third nearest neighbor interactions to obtain a reasonable value of σ. Thus, we have also included them for the top sites for consistency. The resulting interaction parameters are shown in Table III. For each interaction between different types of sites we used the calculated energy per CO molecule ($E_{\text{structure}}$) for a single co-adsorption configuration in the $p(3\times3)$ cell. Each interaction was deduced by: $E_{\text{structure}} = (E_a + E_b + V_{ab})/2$, where E_a and E_b refer to the adsorption energy of the two different binding sites (Table II) and V_{ab} is the parameter describing the interaction between the two sites of different type. The calculated frequencies at low coverage (1/9 ML) are compiled in Table IV. The top site frequencies agree reasonably well with experimental data and previous DFT calculations for 1/3 ML [34]. Until very recently [18], only one peak in the typical on-top region was observed by IRAS experiments [10, 17] for coverages exceeding 1/3 ML, indicating either strong coupling and/or a very low infra red intensity of the molecules adsorbed in non atop sites. On the other hand, hollow and bridge sites have been inferred from Helium scattering experiments, but the precise values of their frequencies cannot be determined at the present time [13]. However, our calculated stretch frequencies for hcp and bridge sites are in good qualitative agreement with previous DFT calculations at 1/3 ML that have their stretch frequencies at 1800 cm^{-1} and 1885 cm^{-1} respectively [34].

As can be seen from Table III, one has such a small binding difference between top and hcp sites that at desorption temperatures (T > 300 K) a significant (greater than 0.1 ML) population of hcp sites below 1/3 ML occurs, completely at odds with experiment. The resulting isobars from these interaction parameters and frequencies [33] is shown in Figure 2a, with an adjustment of the binding energy of -174 meV (the same shift needed for the TPD spectra). At first glance, the curves seem to agree well with the experimental data points included in the figure. However, a closer investigation reveals, that the inflection at 1/3 ML is not captured correctly in the calculation. This disagreement is more clearly seen when the resulting isosteric heat of adsorption is calculated from these isobars using the ASTEK software [36]: the calculated heat of adsorption does not rise at 1/3 ML unlike experiment which rises from $\sim$ 155 kJ/mol to over 180 kJ/mol at 1/3 ML as seen in Figure 2b. This is a consequence of having a significant population of hcp sites below 1/3 ML. It has been argued [33] that the experimental value of the heat of adsorption is too high by about 8 kJ/mol at 1/3 ML, but this does not improve significantly the agreement with our calculations. A similar disagreement occurs for the TPD spectra (Figure 1c) when using the same sticking coefficient as with top sites only: The absence of a significant rise in the heat of adsorption at 1/3 ML is reflected in a shallower minimum in the desorption rate around 440 K for initial coverages greater than 1/3 ML. Correspondingly, the calculated rate, at around 450 K, does not peak as sharply as in experiment. (The small spike in the desorption rate at 430 K results from a small change in the chemical potential at this coverage (0.36 ML). An examination of the *calculated* sticking coefficient [3] here shows that this spike will be eliminated in a full model calculation.) Moreover, the binding difference between fcc and top sites is much larger than between hcp and top sites. This excludes a $(2\sqrt{3} \times 2\sqrt{3})R30^\circ$ structure, for which equal population of hcp and fcc sites has to occur at 1/2 ML.

We also remark that the inflexion point at 1/2 ML for both pressure isobars is due to a (4×2) structure with equal populations of hcp and top sites. This ordered structure is reflected in the rise of the heat of adsorption and its subsequent sharp drop to about 50 kJ/mol around 0.55 ML. In the TPD spectra the peak at 390 K confirms the presence of the (4×2) structure. However, because of fluctuations in the calculated chemical potential at this coverage and temperature we have estimated the height of the peak to have an uncertainty of 20 %. On a more positive note, DFT calculations seem to agree with LEED experiments that suggest that the hollow sites have a binding energy between that of the top sites and the bridge sites, the latter been calculated to have a binding difference with respect to the top sites of 147 meV (obtained from the adsorption energy per CO molecule at 1/9 ML giving −1.649 eV). Finally, we note that the third nearest neighbor interaction between top and hollow sites is attractive which does favor the $(2\sqrt{3} \times 2\sqrt{3})R30^\circ$ structure, but which is not sufficiently large to give it.

V. CONCLUSIONS

The phase diagram and TPD spectra were calculated from first principles and, apart from a difference in overall binding energy, agree well with experimental findings up to 1/3 ML if only top sites are included in a lattice gas model. To model the system beyond 1/3 ML we included top and three fold hollow sites. The resulting

TABLE III: On-site (V_0) and interactions energies (V_1,V_2,V_3,V_{lt},V_{bt},V_{tt}) in (eV) to model the CO/Ru(0001) system with top, hcp and fcc sites using method A together with the corresponding standard deviation (σ). In the second part interaction energies between sites of different type are compiled.

site	V_0	$\Delta E^{\rm top}_{\rm site}$	V_1	V_2	V_3	V_{lt}	V_{bt}	V_{tt}	σ (meV)
top	1.796	-	0.220	-0.010	0.001	0.008	0.014	-0.061	2
hcp	1.750	0.046	0.240	-0.001	-0.008	0.034	0.006	-0.102	3
fcc	1.672	0.124	0.225	-0.001	0.004	0.015	0.003	-0.088	3

sites	V_1	V_2	V_3
distance	$\sqrt{3}/3$	$2\sqrt{3}/3$	$\sqrt{21}/3$
top-hcp	∞	0.049	-0.017
top-fcc	∞	0.046	-0.014
hcp-fcc	∞	0.044	0.004

TABLE IV: Frequencies (cm^{-1}) at 1/9 ML coverage obtained within the DFT framework (method A) together with experimental results from Refs. [13, 19].

Site	ν_x	ν_y	ν_z	ν_{vib}	ν_{rot}
top	46.0	40.4	392.7	1989	378.7
exp. (1/3 ML)	46.0	46.0	445.0	2025	413.0
bridge	163.0	41.8	344.3	1789	170.9
fcc	95.3	62.9	300.6	1759	158.3
hcp	149.8	140.7	313.3	1720	196.1

binding difference between hollow and top sites was determined to be too small to reproduce the isobars and heat of adsorption and, because of the non-zero binding energy difference between hollow sites, does not reproduce the $(2\sqrt{3} \times 2\sqrt{3})R30^\circ$ as observed in LEED experiments. These results seem to indicate that present GGA functionals are able to reproduce the interaction between same adsorption sites, but in order to describe the energy differences between different adsorption sites further improvement is necessary. This shortcoming is not only limited to the CO/Ru(0001) system, but is well known for CO adsorption on transition metals in general [4, 5]. The reason for this is an insufficient description of the energy difference between the highest occupied ($2\pi^*$) and the lowest occupied molecular orbital (5σ) of the CO molecule, which contribute with different intensity at various adsorption sites. Hence, inter-site energy differences are affected. Recently, first attempts have been undertaken to cure this problem and the results look very promising [6].

VI. ACKNOWLEDGMENTS

One of the authors (JSM) would like to thank WestGrid of Canada for the use of their computer resources as well as the Sumner foundation and the National Science and Engineering Research Council of Canada for financial support.

[1] C. Stampfl, H. J. Kreuzer, S. H. Payne, H. Pfnür and M. Scheffler, Phys. Rev. Lett. **83**, 2993 (1999).
[2] J.-S. McEwen, S. H. Payne and C. Stampfl, Chem. Phys. Lett. **361**, 317 (2002).
[3] J.-S. McEwen, S. H. Payne, H. J. Kreuzer, M. Kinne, R. Denecke, H.-P. Steinrück, Surf. Sci. **545**, 47 (2003).
[4] P.J. Feibelmann, B. Hammer, J.K. Nørskov, F. Wagner, M. Scheffler, R. Stumpf, R. Watwe, and J. Dumesic., J. Phys. Chem. B **105**, 4018 (2001).
[5] M. Gajdos, A. Eichler, J. Hafner, J. Phys.: Condens. Matter **16**, 1141 (2004).
[6] G. Kresse, A. Gil, and P. Sautet, Phys. Rev. B **68**, 073401 (2003).
[7] H. Pfnür, G. Michalk, W. Moritz and D. Menzel, Surf. Sci. **129**, 92 (1993).
[8] H. Pfnür, D. Menzel, Surf. Sci. **148**, 411 (1984).
[9] E. D. Williams, W. H. Weinberg, Surf. Sci. **82**, 93 (1979).
[10] H. Pfnür, D. Menzel, F.M. Hoffmann, A. Ortega and A. M. Bradshaw, Surf. Sci. **93**, 431 (1980).
[11] H.-P. Steinrück, private communication.
[12] H. Pfnür and H. J. Heier, Ber. Bunsenges. Phys. Chem. **90**, 272 (1986).
[13] J. Braun, K. L. Kostov, G. Witte and Ch. Wöll, J. Chem. Phys. **106**, 8262 (1997).
[14] H. Pfnür, P. Feulner and D. Menzel, J. Chem. Phys. **79**, 4613 (1983).
[15] S. Kneitz, J. Gemeinhard and H.-P. Steinrück, Surf. Sci. **440**, 307 (1999).
[16] H. Pfnür and D. Menzel, J. Chem. Phys. **79**, 2400 (1983).
[17] G. E. Thomas, W. H. Weinberg, J. Chem. Phys. **70**, 1437 (1979).
[18] P. Jacob, J. Chem. Phys. **120**, 9286 (2004).
[19] P. Jakob, J. Chem. Phys. **108**, 5035 (1998).
[20] H.J. Kreuzer and S. H. Payne, *Computational Methods in Surface and Colloid Science*, (Marcel Dekker, 2000).
[21] D. P. Landau, Phys. Rev. B. **27**, (1983) 5604.
[22] P. Piercy, K. De'Bell, H. Pfnür, Phys. Rev. B **45**, 1869 (1992).
[23] O.G. Mouritsen, *Computer Studies of Phase Transitions and Critical Phenomena*, (Springer, Berlin, 1984).
[24] D. P. Landau, Phys. Rev. Lett. **28**, 449 (1972).
[25] D. P. Landau and K. Binder, *A Guide To Monte Carlo*

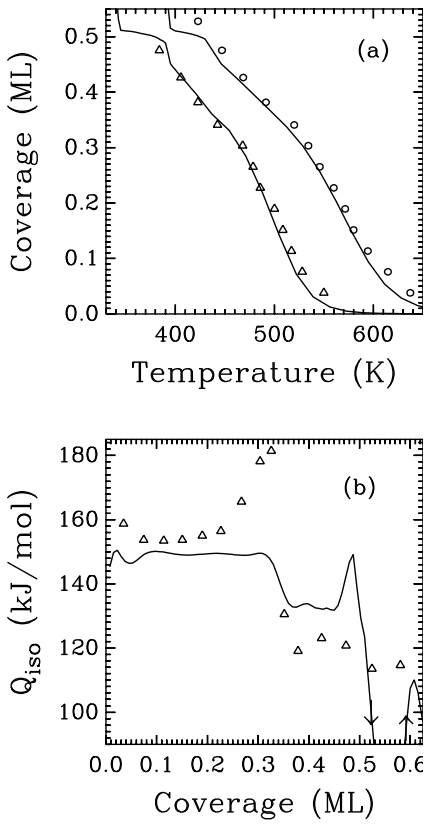

FIG. 2: (a) The predicted isobars from a lattice gas model calculation with top and hollow sites with interactions calculated from DFT (solid curves) compared with experiment at pressures of 1.3×10^{-4} mbar (circles) and 1.3×10^{-6} mbar (triangles). The binding energy of the isobars has been shifted by -174 meV in order to aid with the comparison with experiment. (b) The resulting isosteric heat of adsorption (solid curve) from the same model calculated from the isobars and compared with experiment (triangles) [14].

Simulations in Statistical Physics, (Cambridge University Press, Cambridge, 2000).
[26] B. Widom, J. Chem. Phys. **39**, 2808 (1963).
[27] G. Kresse, J. Furthmüller, Phys. Rev. B **54**, 11169 (1996).
[28] G. Kresse, J. Furthmüller, Computat. Mat. Sci. **6**, 15 (1996).
[29] `http://cms.mpi.univie.ac.at/vasp/`
[30] G. Kresse, D. Joubert, Phys. Rev. B **59**, 1758 (1998).
[31] J. P. Perdew, J. A. Chevary, S.H. Vosko, K.A. Jackson, M.R. Pederson, D.J. Singh, C. Fiolhais, Phys. Rev. B **46**, 6671 (1992).
[32] K. Nagai, K. H. Bennemann, Surf. Sci. **260**, 286 (1992).
[33] S. H. Payne, Jun Zhang and H. J. Kreuzer, Surf. Sci. **264**, 185 (1992).
[34] J. J. Mortensen, Y. Morikawa, B. Hammer and J. K. Nørskov, Z. Phys. Chem. **198**, 113 (1997).
[35] C. Stampfl, M. Scheffler, Phys. Rev. B **65**, 155417 (2002).
[36] `http://fizz.phys.dal.ca/~kreuzer/astek.html`